SPATIAL AND ENVIRONMENTAL INFLUENCES ON THE ASSEMBLY OF SILK MICROBIOMES IN A SOCIAL SPIDER

Authors

Kara J.M. Taylor[1]*, Steven T. Cassidy[1], Peter R. Marting[2], Mathew A. Leibold[1,3], Carl N. Keiser[1]

Affiliations

1. Department of Biology, University of Florida, Gainesville, FL 32611
2. Department of Biological Sciences, Auburn University, Auburn AL 36849
3. Institut Natura e Teoria en Pireneus, Surba, France

*Corresponding author

k.taylor2@ufl.edu

SUMMARY

In nesting animals, the built environment can play an important role in host-associated microbiome assembly. However, the sources and processes structuring the resulting microbiome remain underexplored. In the social spider *Stegodyphus dumicola,* philopatric sisters collectively build and maintain a silken nest, capture prey, and exhibit alloparental care. We used *S. dumicola* as a test system to assess the source and spatial/environmental processes structuring the nest microbial communities. We collected paired silk and soil samples along two orthogonal transects in southern Africa. Bacterial and fungal communities were extracted using high-throughput sequencing of 16S-rRNA and ITS barcoding genes and assessed using the SourceTracker tool for R, distance-based regression of soil and silk dissimilarity, and variation partitioning. Silk bacteria were partially derived from soil bacteria, but there is no apparent difference in the contribution of local vs. non-local soils: nest microbial communities are no more similar to microbes in the local soil beneath them than soil found hundreds of kilometers away. In contrast, silk fungi receive few taxa from the soil community but show a stronger relationship with local over non-local soils. Silk bacterial communities are weakly structured by spatial and environmental processes, (i.e. dispersal and abiotic filtering) suggesting low dispersal limitation and a stronger influence of ecological drift. Silk fungal communities, in contrast, indicated stronger associations with spatial and environmental processes. The large contribution of extrinsic sources to the nest microbiome suggests high immigration potential for opportunistic or harmful microbes that may be partly responsible for eventual colony collapse.

Keywords: Community ecology, bacteria, fungi, *Stegodyphus dumicola*

Introduction

Social animals that create permanent living structures maintain dispersal feedback between themselves and their built environment, which accumulate and structure host-associated microbiota (Hill & Gilbert 2023; Li *et al.* 2021; Miller *et al.* 2018). In extreme cases, the built environment is manipulated by hosts to specifically select for essential mutualistic microbes (Lucas *et al.* 2019). However, in most cases, nest-associated microbes are not obligate symbionts of the host. This means that the built environment (i.e., nest) can act as an equal-opportunity source for potential host-associated microbes dispersing from other origins – vital mutualists, indifferent commensals, and virulent parasites alike. Thus, the microbial metacommunity formed by the social group (the 'social microbiome'; (Sarkar *et al.* 2020)) is likely to be affected by extrinsic sources that facilitate taxa colonizing the nest. Accumulation of extrinsically sourced taxa in the nest may have short- and long-term effects on the health of the social group (Sarkar *et al.* 2024).

Social spiders use their nests as all-purpose living spaces for prey capture, feeding, mating, brood care, and shelter from predators across multiple generations (Aviles 1997). Colonies undergo boom-and-bust cycles, with most collapsing within three to five years for unknown reasons (Busck *et al.* 2022; Crouch & Lubin 2001). Colonies are comprised of two main components: the central silken domicile (retreat) and the surrounding capture web. Retreats are constructed with combinations of tough sheet and tangle webs that contain plant matter, soil/sand, carapaces, arthropod pieces, whole insect corpses, and assemblages of live arthropods (Fernandez-Fournier & Avilés 2018). Some species build retreats that create distinct microhabitats with much hotter conditions than their surroundings (Soydaner 2013). In contrast, capture webs contain very sticky silk in less dense combinations of tangle and sheet silk. Capture silk is susceptible to damage from rain, debris, and insects which appears to be replaced/repaired at a higher rate than retreats (Ainsworth *et al.* 2002; Christenson 1984). Due to their inherently different functions and structural properties, retreat and capture silk are expected to house different microbial communities.

African social spiders (*Stegodyphus dumicola*) harbor microbiomes in their bodies, on their cuticle, and in their silken colonies. Their retreats are composed of extremely tough cribellate silk with crisscrossing tunnels and contain one or more capture webs that radiate from the retreat as mostly two-dimensional structures. Although this species is broadly distributed across southern Africa, it is notable for exhibiting high philopatry and inbreeding and infrequent dispersal (Settepani *et al.* 2017; Smith *et al.* 2009). These behaviors may partly explain the high microbiome similarity among spiders within the same nest compared to spiders from other nearby nests (Busck *et al.* 2020). However, individuals that do engage in long-distance dispersal vial "ballooning" establish new nests ('founders') can experience ecological drift in their microbiota (Rose *et al.* 2023a), in part due to loss of socially maintained taxa and acquisition of novel environmental microbes during dispersal. This suggests that extrinsic sources of microbiota are likely to constitute a large proportion of the nest microbiota as well.

The nearby sandy soil is but one source of potential colonists: the movement of wind-borne debris also assists microbial dispersal and can also homogenize built microbiomes over greater distances. Interestingly, previous microbiome analyses of *S. dumicola* and their silken nests have shown only weak spatial compositional turnover patterns (i.e. distance-decay) except at very large spatial scales (>500km; (Keiser *et al.* 2019; Nazipi *et al.* 2021)). Silk fungal communities, on the other hand, have demonstrated compositional turnover at smaller spatial scales than bacteria (Nazipi *et al.* 2021). It is possible that soil microbes do strongly influence silk microbiomes, but

soil bacteria and fungi contribute to different degrees. Bacterial and fungal taxa contributed by soil may be extremely variable in their dispersal capabilities: even a low degree of dispersal limitation can induce a distance-decay pattern. However, if dispersal is sufficiently unlimited, nearby sites may not be easily differentiable from distant sites.

The distribution of African social spider colonies across a large geographic range and a mild aridity gradient makes this a great system to test assembly rules of the built microbiome in a natural setting. Here, we explored the impact of an extrinsic microbial source (the soil) on the microbial community structure of actively occupied built environments (retreat and capture silk) utilized and maintained by *S. dumicola*. Taking the 'metacommunity perspective' means we consider the possible assembly outcomes of microbial dispersal between patches at both local and regional scales simultaneously (Leibold & Chase 2017). We use a combination of SourceTracker analysis (Knights *et al.* 2011), variation partitioning (Legendre 2008), and classic distance-decay methods to tease apart answers to the following questions: 1) To what degree does soil microbiota influence the microbial community associated with *S. dumicola* colonies? 2) Is the relationship between silk and soil microbiota distance-dependent? 3) Do abiotic factors (temperature and aridity) interact with dispersal limitation to influence the assembly of silk microbiota? 4) How do these patterns differ between communities of bacteria and fungi? By exploring these patterns in both bacterial and fungal communities, we can better understand how these two microbial groups experience community assembly within the built environment of a highly social species. The results highlight the influence of extrinsic soil microbes on silk microbial composition; however, quantifying the effects of specific extrinsic taxa on host or nest health is outside the scope of this analysis.

Methods

Study design and sample collection

In December 2018, we collected samples along two roadside transects that experience a similar rate of environmental change (temperature and aridity) along their lengths (Figure 1a). The East-West transect follows the N10, N14, and R31 highways in South Africa, and the North-South transect follows along the B1 highway in Namibia (Figure 1b). Mean annual temperature and precipitation were gathered from WorldClim v2 30 arcsecond (~1km) raster files (Fick & Hijmans 2017). Aridity data was gathered from the CGIAR-CSI Global-Aridity and Global-PET Database (Zomer *et al.* 2007, 2008). All climatic variables were cross-referenced with the GPS coordinates of each site location using QGIS (QGIS Development Team & others 2024).

We collected two silk types (retreat and capture) from S. dumicola colonies as well as soil samples from immediately below each colony (Figure 1c). We collected capture silk samples by twisting a sterile cotton swab in each capture web to gather up approximately 0.5 mL of mechanically sticky silk and placing it into 1.5 mL centrifuge tubes. We used sterile plastic forceps to remove approximately 10 mL of retreat silk and placed it into sterile 15 mL tubes. To collect soil, we scooped approximately 10 mL of sandy soil, no deeper than 5 cm, into sterile 15 mL tubes directly below each colony. We filled all samples to the max fill line on each tube with RNA*later*® (Sigma-Aldrich, St. Louis, MO) for transport and storage. Samples were then transported to the University of Florida and placed in a -20ºC freezer prior to processing.

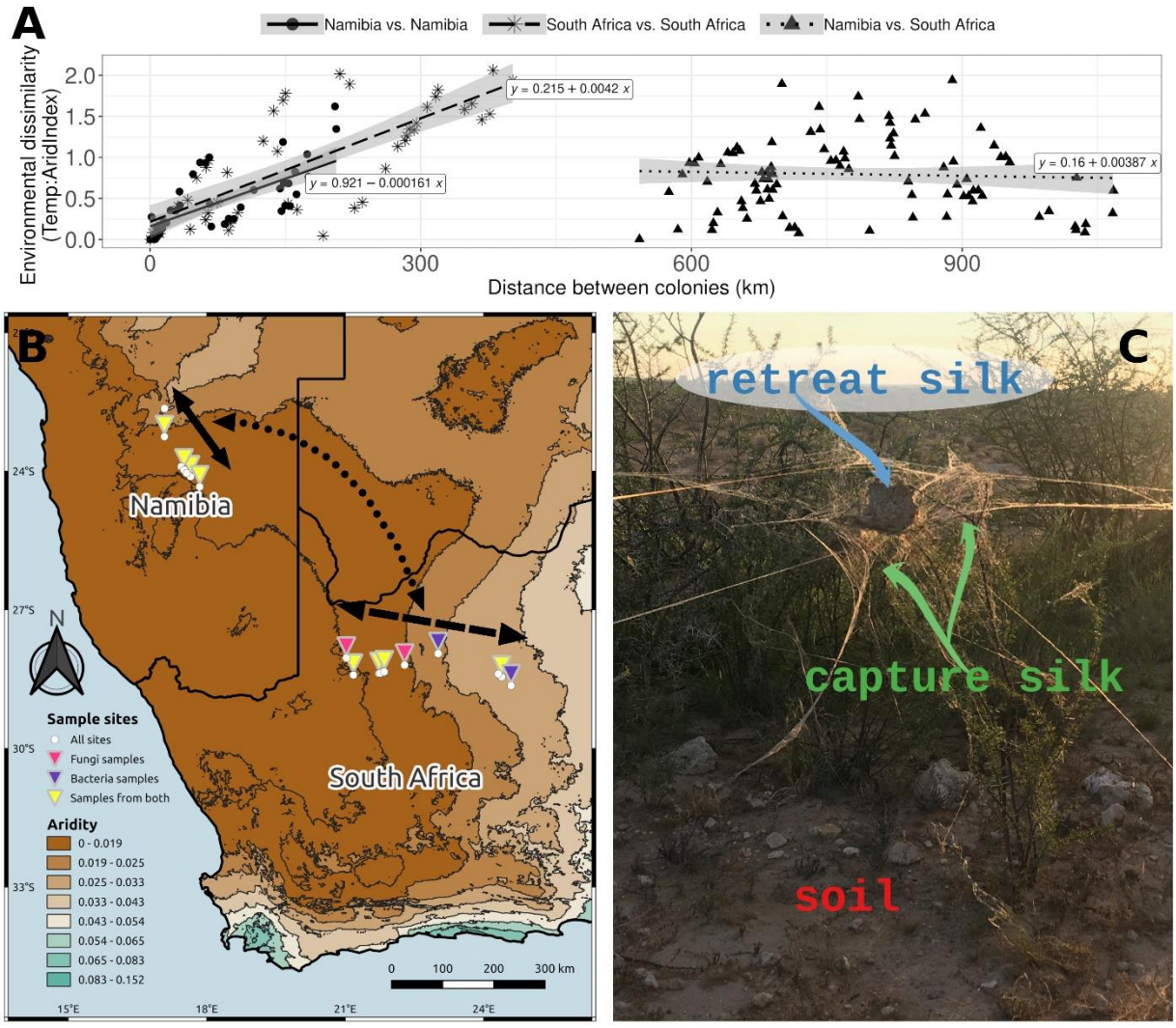

Figure 1. Silk and soil collection along a temperature and aridity gradient in southern Africa. *A) Pairwise relationship of geographic distance and environmental dissimilarity. Environmental dissimilarity is measured as Euclidean distance based on mean annual temperature and aridity. Pairwise comparison of sample sites is made within-transect (Namibia or South Africa) or between-transects (Namibia vs South Africa). B) Map of the sampling area. Samples from all sites (white dots) were used to calculate alpha and beta diversity metrics. Downstream analysis is restricted to the 13 sites labeled Fungi (pink), Bacteria (purple), or both (yellow). At these sites, all three sample types (retreat, capture, soil) were successfully sequenced. C) Example site showing all three sample types.*

To prepare samples for DNA extraction, we thawed each sample tube, removed the RNA*later*® at the top of the tube, and centrifuged them 3 times at 4500 rpm for 5 mins. to separate and remove RNA*later*® supernatant from the sample as much as possible. Once RNA*later*® was removed, we added 0.01 M of phosphate buffered saline solution (-0.138M NaCl mixed with 0.0027 M KCl at pH 7.4). For capture silk samples, we used sterile forceps to remove the capture silk from the cotton swap used to collect the silk and placed the silk in a new sterile 1.5 mL tube.

All samples were vortexed at the end and frozen at -20ºC. We sent all samples to ZymoBIOMICS Targeted Sequencing Service (Zymo Research, Irvine, CA) for processing and sequencing.

DNA extraction, sequencing, and HTS data processing

ZymoBIOMICS-96 MagBead DNA Kit (Zymo Research, Irvine, CA) was used to extract DNA using their automated platform. Bacterial 16S ribosomal RNA gene targeted sequencing was performed using the Quick-16S™ NGS Library Prep Kit (Zymo Research, Irvine, CA) which amplifies the V3-V4 region of the 16S rRNA gene. Fungal ITS gene targeted sequencing used the same library prep kit but with ITS2 primers substituted for 16S primers. The ZymoBIOMICS Microbial Community Standard (Zymo Research, Irvine, CA) was used as a positive control and negative controls (i.e., blanks with no DNA) were included to assess the level of contamination for each DNA extraction during the library prep.

Real-time PCR was used to amplify the DNA and quantified with qPCR fluorescence readings, which were pooled together based on equal molarity. The final pooled library was cleaned with the Select-a-Size DNA Clean & Concentrator (Zymo Research, Irvine, CA), then quantified with TapeStation (Agilent Technologies, Santa Clara, CA) and Qubit (Thermo Fisher Scientific, Waltham, WA). The final library was sequenced on Illumina MiSeq with a v3 reagent kit (600 cycles). The sequencing was performed with 10% PhiX spike-in.

A qPCR was set up using the same primers as the library prep with a standard curve made with plasmid DNA for both 16S and ITS2 sequences in 10-fold serial dilutions. The standard curve was used to calculate the number of gene copies in the reaction for each sample. The number of gene copies per µL was calculated using the PCR input volume (2µL) for each DNA sample. The number of genome copies per µL DNA sample was calculated by dividing the gene copy number by an assumed number of gene copies per genome (i.e., 4 16S copies per genome and 200 ITS copies per genome). The assumed genome size used to for this calculation was 4.64 x 106 bp, the genome size of Escherichia coli, for 16S samples, and 1.20 x 107 bp, the genome size of Saccharomyces cerevisiae, for ITS samples. The full calculation for this is in the Appendix.

Data analyses

For both bacterial and fungal datasets independently, general metrics of diversity and composition were calculated using the full sample set. However, SourceTracker, distance-decay, and structuring process analysis were performed on a subset of sites from which data was successfully collected from all three sample types. In both bacterial and fungal datasets, all three sample types were represented from 12 sites, but one site was removed from each dataset due to poor or biased sampling, leaving samples from 13 total sites across both datasets (2 bacteria-only, 2 fungi-only, 9 with both; Figure 1b). All analyses were conducted in Rstudio using R version 4.4.1 (R Core Team 2024).

Sample diversity and composition

To help visualize ASV distribution among sample types, ASVs were parsed based on their presence in at least one sample of any type (soil, capture, or retreat). An ASV can be found in any of the seven possible combinations for the three sample types (i.e. soil, capture, retreat, soil & capture, soil & retreat, retreat & capture, soil & capture & retreat). For each sample, the total ASV relative abundance (%) is given for each sample type combination.

Basic diversity analyses were also conducted to assess sampling differences between sample types. Species accumulation curves were drawn to assess the adequacy of sampling depth for all samples (`vegan`: (Oksanen *et al.* 2022)). Three alpha diversity metrics (Shannon's H [`vegan`], absolute richness [`vegan`], Faith's phylogenetic diversity [PD; `picante`: (Kembel *et al.* 2010)]) and Pielou's evenness were used to examine within-sample diversity and compare between sample types. Statistical differences between sample types were assessed with ANOVA and the Tukey HSD post-hoc test. Principal coordinates and distance-based PERMANOVA were used to examine compositional differences between sample types (`pairwiseAdonis`: (Martinez Arbizu 2020)). Beta dispersion was used to assess the degree of within-sample type similarity (`vegan`) and differences between sample types were assesed with ANOVA and Tukey HSD.

Structuring processes

The compositions of most microbial communities in nature are structured by both deterministic and stochastic processes (Martiny *et al.* 2006), and structural turnover can occur along both spatial and environmental gradients (Feng *et al.* 2019; Gilbert & Lechowicz 2004; Ranjard *et al.* 2013). Confounding of spatial and environmental effects is common and several methods exist to approach this problem, including linear regression and the Mantel test (Astorga *et al.* 2012), phylogenetic null models (Stegen *et al.* 2012), and variation partitioning (Peres-Neto & Legendre 2010). Each of these methods has its uses and applications that are appropriate for different kinds of sampling design. In this case, we have two transects across similar environmental gradients, and we can draw comparisons from within and between them to separate very long distance effects from environmental effects. We know that the two transects share a similar environmental gradient to distance relationship (Figure 1a). We also know that there may be little spatial structure for the silk microbiome of *S. dumicola* at scales <500km (e.g., within the transects; (Nazipi *et al.* 2021)); however, pairwise comparisons between sites of different transects can separate whether compositional dissimilarity is due to environmental difference or large-scale dispersal limitation. Here, we begin with distance-decay regression (Soininen *et al.* 2007) and add in environment-decay multiple regression for comparison (e.g. (Locey *et al.* 2020; Ranjard *et al.* 2013)). We then use variation partitioning to estimate how much variation is attributed to the environmental gradient, to the spatial gradient, and to spatial autocorrelation effects present in the environmental gradient (Legendre *et al.* 2005; Peres-Neto *et al.* 2006).

The distance-based approach used binary Bray-Curtis distances between samples of the same type regressed against geographical distance and 'environmental distance,' respectively. Compositional distance was calculated as $\frac{A+B-2J}{A+B}$ where A and B are the number of taxa in each sample and J is the number of taxa in both (Oksanen *et al.* 2022). Only taxa present in more than one sample were included (i.e. singletons were removed). Environmental distance was calculated as the Euclidean distance between sites based on temperature and PET. Both temperature and PET covariates were centered and scaled prior to this calculation. Likewise, geographical distance was calculated as the Euclidean distance between sites from latitude and longitude given in decimal degrees. Geographical distances were converted from decimal degrees to kilometers after calculation. Environmental and geographical distance multiple regressions were performed for within- and between-transect comparisons with compositional distance.

To perform variation partitioning, we first constructed a Moran's Eigenvector Map (MEM) from a spatial weighting matrix of the input site coordinates (`adespatial`: (Guénard & Legendre 2022)), following Dray et al (Dray *et al.* 2006). MEM1 was highly correlated with site geographic

location and best accounted for the degree of spatial segregation of the two transects. The MEM was first used to quantify the degree of spatial autocorrelation present in the environmental covariates, temperature and PET). MEM2 was highly correlated with both environmental variables and best represented the environmental gradient present in both transects. Therefore, MEM1 was used as the spatial factor during variation partitioning in order to separate large-scale regional effects from within-transect effects. A Moran Structural Randomization (MSR) test (`adespatial`) was then performed between temperature and PET to quantify the degree of correlation between the covariates after accounting for spatial autocorrelation. The MSR test indicated that, after accounting for inherent correlation due to spatial autocorrelation, temperature and PET were sufficiently non-correlated to include both in subsequent variation partitioning analysis (`vegan`). Statistical significance of the environmental and spatial components was quantified using canonical correspondence analysis (CCA; `vegan`).

SourceTracker

SourceTracker analysis (Knights *et al.* 2011) is a Bayesian approach to quantifying the proportion of a microbial population in a sample that comes from each of a set of sources identified a priori. Originally, it was designed as a tool for identifying sources of contamination in microbiome samples. It randomly assigns each ASV to one of the given source environments and updates the likelihood of observing it in that source based on the proportion present in the sink environment. It repeats this Gibbs sampling process 10 times to estimate the variability of the posterior distribution. We used SourceTracker v1 (https://github.com/danknights/sourcetracker), which was written for implementation in R (Knights 2016).

After each sink ASV has been assigned proportionally to each source, we took the mean of the Gibbs samples of the ASV for each sample. We then took the mean across the samples to get an estimate of the overall proportional source assignment for the sequence. With each capture silk ASV given an assignment to 'soil', 'retreat' or 'unknown' source, we used these proportions to group sequences by source value majority. Four groups were created: Soil, Retreat, Mixed, and Unknown. ASVs grouped into the Soil, Retreat, and Unknown clusters were those assigned to each of those three sources by SourceTracker with a proportion greater than 50%. ASVs grouped into the 'Mixed' cluster were those with proportions less than 50% for all three assigned sources.

Variation between Gibbs draws of an ASV in each sink sample is quantified as the coefficient of variation ($CV = \sigma/\mu$). The skewness and kurtosis of the CV distribution for each source summarizes the degree of uncertainty around draws from each source. Skewness > 1 and high kurtosis indicates strongly right-skewed data that peaks near CV=0. Skewness <1 and low kurtosis indicates weakly right-skewed data that peaks further from CV=0.

Intra-colony similarity

To better understand the SourceTracker results, we also examined compositional turnover between sample types as a function of distance. Cross-comparison between the communities of different sample types allows us to see the compositional relationship between sample types and whether the strength of that relationship is affected by the physical distance between samples. Similar to the traditional distance-decay approach, strong distance-dependent turnover between sample types indicates that microbial exchange is more common between nearby samples than distant ones.

Pairwise compositional distance was calculated between each bacterial and fungal dataset and categorized by geographical distance between the sample collection sites. We calculated binary

Bray-Curtis distances (`vegan`) between retreat and capture matrices, between retreat and soil matrices, and between capture and soil matrices. We included only those taxa that were present in more than 1 sample of either type (singletons removed).

We first performed multiple regression of pairwise compositional distances between samples against the geographical distances within and between transects. We then grouped compositional distances by relationship: between samples collected from the same site ("within-colony"), between samples of different types from the same transect ("within-transect"), and between samples of different types between transects ("between-transect"). The mean compositional distances for each group were compared using two-way ANOVA. In this way, we can test whether the microbiota collected from silks of the same colony are more similar to each other than to silks of more distant colonies (i.e. distance-decay); likewise, we can test whether local soils contribute to silk microbiome composition more than distant soils.

Data accessibility

Community feature tables, sample metadata, and data analysis pipeline are available at https://github.com/kjmtaylor22/stegodyve, which is downloadable as a package using `devtools::install_github`.

Results

Bacterial and fungal DNA extraction and sequencing were successful for 22 soil samples, 12 retreat silk samples, and 21 capture silk samples, though bacterial DNA sequencing was successful for one additional retreat silk sample. The full dataset was used to examine general metrics of diversity and composition. Subsequent analyses were conducted using the 33 sample datasets as described in Methods.

Silk microbial communities are distinct from soil

Sample type (soil vs. retreat vs. capture) had a significant effect on alpha diversity and evenness in bacteria, but not in fungi (Figure 2, Diversity; Figure S2). Bacterial alpha diversity (Shannon's H, richness) was significantly higher in soil than silks (Tukey HSD: padj<0.01), but not different between silk types. Evenness in the soil communities was significantly higher than the retreat communities (Tukey HSD, padj =0.005), but not different from capture communities. Fungal alpha diversity and evenness were not significantly different between the three sample types. Phylogenetic diversity (Faith's PD) was not significantly different between sample types for either bacterial or fungal communities.

Differences in composition among samples (Figure 2, Composition) were explained predominantly by the sample type (soil, retreat, capture) and secondarily by transect (Namibia, South Africa) in both bacteria (PERMANOVA; $p<0.001$) and fungi (PERMANOVA; $p<0.001$). These factors accounted for 21% and 18% of the total variance in bacterial and fungal communities, respectively. In the bacterial samples, all three sample types were compositionally distinct. In contrast, while fungal communities were compositionally distinct between silk and soil, there were no differences between silk types.

Bacterial beta dispersion was not significantly different between sample types. Fungal beta dispersion was significantly higher in soil than retreat silk (Tukey HSD; $p_{adj}=0.003$) and capture silk (Tukey HSD; $p_{adj}=0.002$) and not significantly different between capture and retreat silk (Figure 2, Variability).

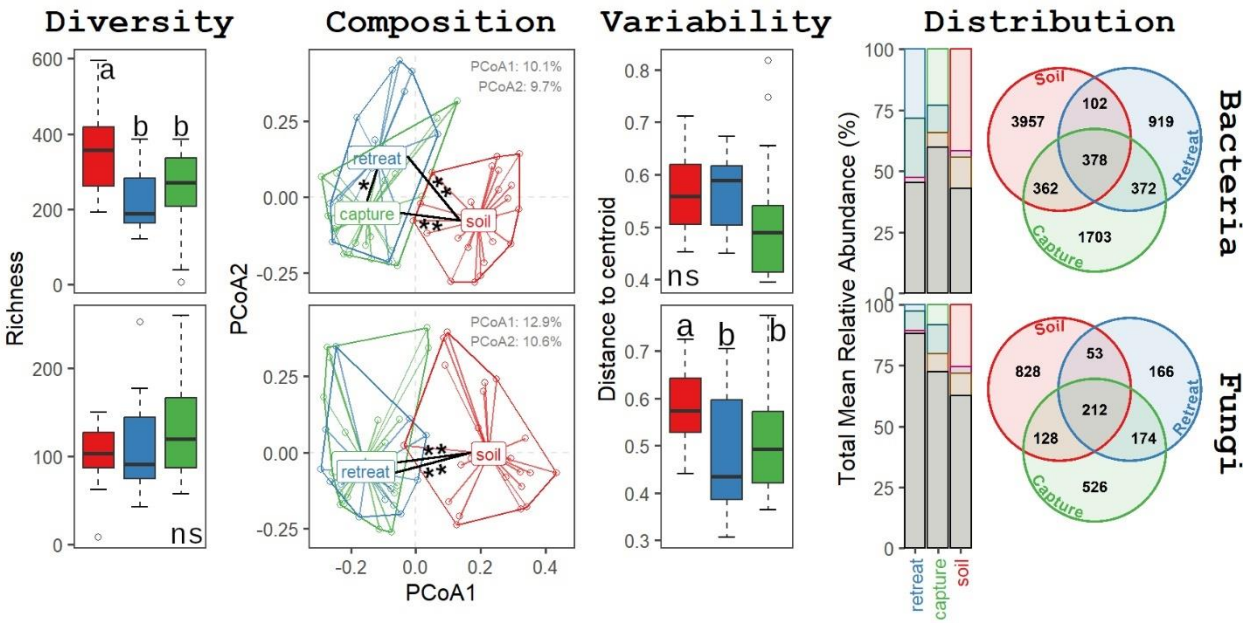

Figure 2. Alpha and beta diversity of microbiota associated with silk and soil samples. *Panels from left to right compare simple metrics of diversity (richness), composition (principal coordinates), variability (dispersion) and taxonomic distribution among sample types for bacterial communities (top) and fungal communities (bottom). Groups that are statistically different from on another are indicated either with letters or stars (*p<0.05; **p<0.01). Non-significant differences are indicated with 'ns.'*

Differences between soil and silk composition were driven largely by the numerical difference in species richness (Figure 2, Dispersion). However, though soil tended to be more species rich, bacterial taxa specific to each sample type or shared among all three sample types were the most abundant. Taxa shared just between soil and retreat silk or soil and capture silk were numerically rare. In contrast, the most abundant fungal taxa were those that were shared among all three sample types or were unique to soil. Taxa shared between just two sample types or unique to silk were more numerically rare.

Silk communities are structured by different ecological processes than soil

Examining compositional turnover against geographical distance alone generally explained compositional turnover well (Figure 3a, Bacteria: retreat R^2 =0.41, F=11.98, p<0.001, capture R^2 =0.26, F=5.92, p<0.001; Figure 3c, Fungi: retreat R^2 =0.49 F=16.43, p<0.001, capture R^2 =0.62, F=27.95, p<0.001). There were no within- or between-transect differences for the different sample types, except in the retreat bacteria where the slopes of the two lines differed (t=2.09, p=0.04). The lack of statistical difference in the multiple regression indicates that the relationship between composition and geographical distance is ultimately the same both within- and between-transects. In absentia of an environmental decay gradient, this might be easily mistaken for evidence of distance-decay patterns. However, compositional turnover across an environmental gradient was also considered:

Environmental effects on composition within and between transects have substantial explanatory power for silk compositional variation (Figure 3b, Bacteria: retreat R^2 =0.44, F=13.13, p<0.001, capture R^2 =0.45, F=13.69, p<0.001; Figure 3d, Fungi: retreat R^2 =0.41, F=11.60,

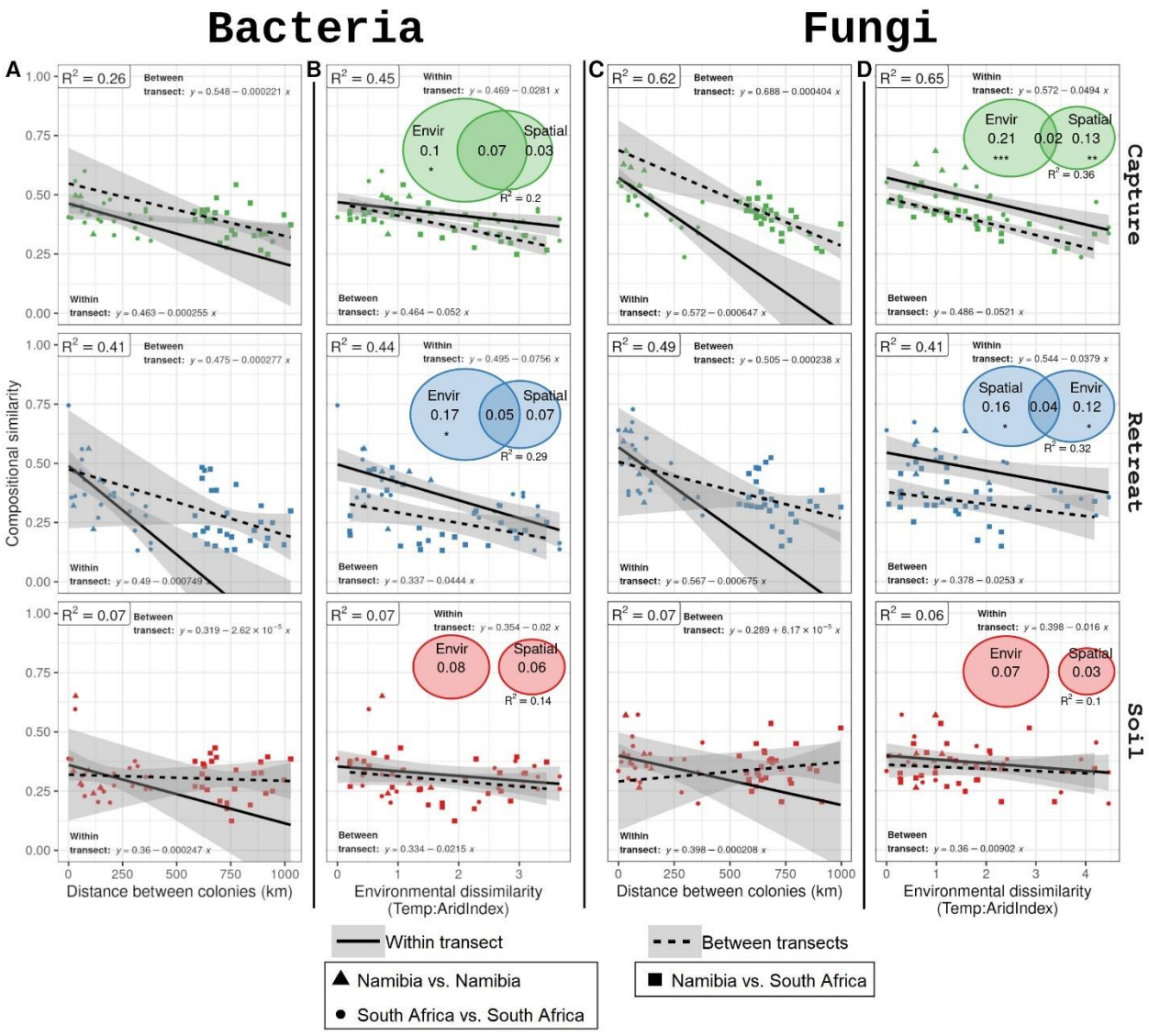

Figure 3. Parsing spatial and environmental processes influencing silk and soil microbial community assembly. *A,B) Bacteria. C,D) Fungi. A,C) Multiple regression of pairwise sample compositional similarity against geographical distance (km). B,D) Multiple regression of pairwise sample compositional similarity against environmental dissimilarity. Environmental dissimilarity is calculated as a Euclidean distance based on mean annual temperature and aridity at each site. Sample pairs are either both from the same transect ("Within transect," solid line) or from different transects ("Between transect," dashed line). Trendline equations are given for each line separately. See Tables S1,2 for coefficients and statistics. B,D insets) Venn diagrams showing the proportion of the total R2 accounted for by environmental and spatial processes. The total R2 is given below the Venn segments. Stars indicate statistical significance based on CCA (*p<0.05, **p<0.01, ***p<0.001).*

p<0.001, capture R^2 =0.65, F=30.99, p<0.001). Generally, sites that were more similar environmentally across transects were also more compositionally similar than those that were more environmentally distinct. Within transects, sites that were more similar environmentally generally

had greater silk compositional similarity (Bacteria: retreat t=-4.72, p<0.001, capture t=-3.32, p=0.002; Fungi: retreat t=-2.60, p=0.01; capture t=-6.16, p<0.001). Interestingly, the between-transect decay trend paralleled the within-transect result but y-downshifted in three of the four silk communities. The y-downshift of the between-transect regression relative to the within-transect regression is significant in the silk fungal communities (Fungi: retreat t=-3.55, p<0.001, capture t=-3.33, p=0.002) but not in the silk bacterial communities (Bacteria: retreat t=-3.09, p=0.003, capture t=-0.19, p=0.85). Neither silk nor soil microbial communities show significant interaction effect between environmental decay and transect (Table S1,2), meaning that environmental influence on compositional dissimilarity is not affected by increasing distance.

Variation partitioning analysis of silk microbial communities showed that silk compositional turnover is more dependent on environmental differences than geographical distance, although the two variables are measurably confounded (Figure 3b, insets). Permutation test for CCA of bacterial silk communities indicates that the environmental component is significant (Retreat: R^2 =0.17, F=2.09, p=0.035; Capture: R^2 =0.1, F=1.56, p=0.021) but the spatial component is not (Retreat: R^2 =0.07, F=1.78, p=0.1; Capture: R^2 =0.03, F=1.27, p=0.2). Overlap between bacterial spatial and environmental components is large relative to the individual fractions (Retreat: R^2 =0.05; Capture: R^2 =0.07). CCA permutation tests for fungal silk communities indicates that both the environmental and spatial components are significant (Retreat: environmental R^2 =0.16, F=1.77, p=0.043, spatial R^2 =0.12, F=2.80, p=0.015; Capture: environmental R^2 =0.21, F=2.44, p=0.001, spatial R^2 =0.13, F=2.55, p=0.003). Overlap between fungal spatial and environmental components is small relative to the individual fractions (Retreat: R^2 =0.04; Capture: R^2 =0.02).

In contrast to the silk, soil microbial composition is poorly explained both by within- or between-transect environmental dissimilarity and by geographical distance alone (Figure 3c,d; R^2 < 0.07). In other words, neither environmental filtering nor geographical distance has a significant impact on soil microbe composition. Similarly, partitioning of soil community variation is weak in both the bacterial and fungal communities (Figure 3d, insets; Bacteria: environmental R^2 =0.08, F=1.41, p<0.1, spatial R^2 =0.06, F=1.56, p<0.1; Fungi: environmental R^2 =0.07, F=1.35, p=0.1, spatial R^2 =0.03, F=1.23, p>0.1). There is no measurable overlap between the environmental and spatial variation components in the soil microbial communities (Figure 3b,d insets, bottom).

Capture silk is a sink for soil bacteria dispersing from across the region

SourceTracker identified 1930/5167 bacterial ASVs and 606/2087 fungal ASVs abundant enough in the capture silk to be drawn by the Gibbs sampler. The goal of this analysis was not to generate an exhaustive catalogue of soil taxa present in the silk; rather, it was to assess the potential for soil to contribute to silk microbiome assembly.

SourceTracker identified several highly abundant soil bacterial ASVs present in the capture silk. The top 5 most abundant bacterial ASVs in capture silk were classified as Retreat or Soil and belong to *Geodermatophilus* and *Modestobacter*. For bacterial ASVs drawn from retreat and soil sources, the distribution of CV of Gibbs draws is highly right-skewed (Figure 4a; skew > 5, kurt > 46). The assignment of bacterial ASVs to an Unknown source generally exhibited greater uncertainty (Figure 4a ; skew=1.46 kurt=5.49). Capture silk bacteria are drawn similarly from soil (764/1930; 39.6%), retreat silk (509/1930; 26.4%), and an unknown source (587/1930; 30.4%).

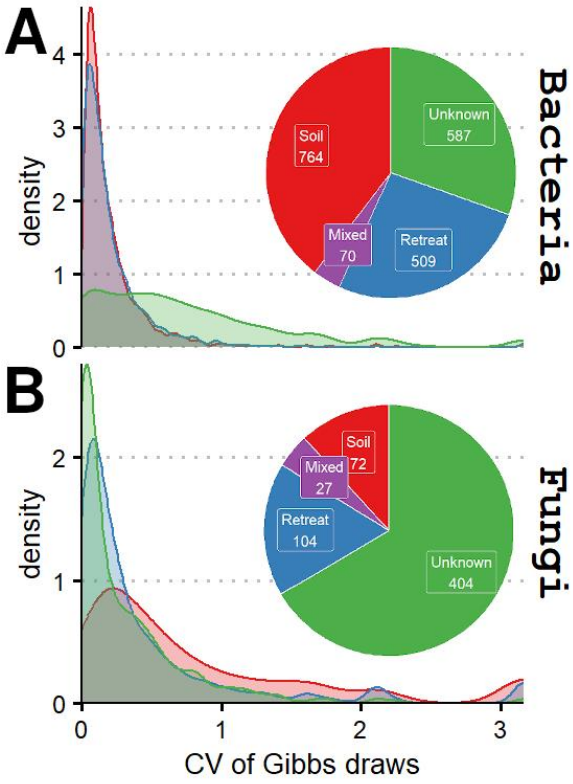

Figure 4. Sources of microbial taxa in capture silk and the uncertainty of source assignment by SourceTracker based on ten Gibbs draws. *Pie charts show the number of ASVs analyzed that were assigned to a given source. Density plots show the distribution of coefficient of variation of assignments for each ASV across the ten Gibbs draws. A) Bacteria. B) Fungi.*

The remaining capture silk bacteria (70/1930; 3.6%) are most likely drawn in part from multiple sources.

In contrast, identifiable soil fungal ASVs were typically rare in capture silk, and the most abundant taxa were either classified as Unknown or Retreat. The top 5 most abundant fungal ASVs belong to *Aureobasidium, Pleosporales*, and *Neocamarosporium*. For fungal ASVs drawn from retreat and Unknown sources, the distribution of CV of Gibbs draws is highly right-skewed (Figure 4b; skew > 2, kurt > 10). The assignment of fungal ASVs to soil generally exhibited greater uncertainty (Figure 4b; skew=1.34, kurt=3.70). Capture silk fungi are largely drawn from an unknown source (406/606; 67.0%). Comparatively few capture silk fungi are drawn from the soil (75/606; 12.4%) and retreat silk microbiota (103/606; 17.0%), and a few are indeterminate (22/606; 3.6%).

Silk is a sink for soil fungi dispersing locally

In the bacterial communities, the distance-decay relationship is generally weak. Compositional similarity of the capture and retreat silk microbiota is significantly higher within colonies than between transects (ANOVA, p=0.003), but the within-colony comparison is not significantly different from comparisons within transect. Similarity between the capture silk and the soil microbiota is slightly higher within colony than within transect (ANOVA, p=0.03) but is

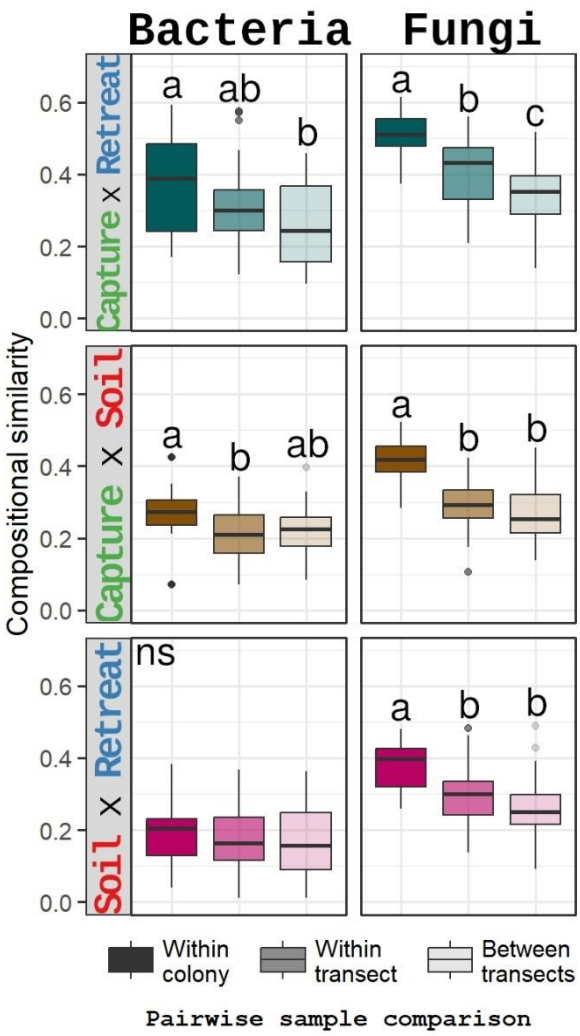

Figure 5. Compositional similarity between sample types is a function of distance between transects. *Samples of different types are generally more similar when taken from the same location ("Within colony") than when taken from different locations ("Within transect" or "Between transects"). Capture silk microbiota are compared with the retreat silk microbiota (teal; top panels) and soil microbiota (brown; middle panels), and retreat silk microbiota are compared with soil microbiota (magenta; bottom panels). Groups that are statistically different from on another are indicated with letters. Non-significant differences are indicated with 'ns.'*

not different from the 'between transect' group. The retreat silk bacterial communities indicate equal compositional similarity to local and distant soil microbiota.

In contrast, the fungal communities indicate a strong distance-decay relationship between samples collected at the same site versus samples collected further apart. Compositional similarity between capture and retreat silk samples collected from the same site is strongly differentiated from samples collected within transect (ANOVA, $p<0.002$) and from samples collected between transects (ANOVA, $p<0.001$). There is also a significant difference in compositional similarity between samples collected within and between transects (ANOVA, $p=0.002$). Similarly, both the capture and retreat silk microbiota show significantly stronger similarity to local soil than soils of

the same transect (ANOVA, $p<0.001$ and $p=0.015$, respectively) or to soils of the other transect (ANOVA, $p<0.001$ and $p<0.001$, respectively).

Discussion

Built environments act as reservoirs for host-extrinsic microbiota and host-associated microbiota alike (Bosch *et al.* 2024; Wilkins *et al.* 2016). In a metacommunity mindset, these reservoirs engage in dispersal feedbacks with the host that can reinforce existing host microbiota and/or facilitate transmission within the social group (Miller *et al.* 2018; Sarkar *et al.* 2020). For social spiders, a potentially major source of extrinsic microbiota is the sand and soil being blown around the arid landscape of Southern Africa. Both the capture and retreat silk are typically suspended in bushes and trees and easily accumulate soil and dust particulates as well as other debris. Although transmission rates from the environment are likely lower than transmission rates among individuals, environmental acquisition by one member of the social group has the potential to be passed quickly among nestmates for both fungi (Cassidy *et al.* 2025) and bacteria (Keiser *et al.* 2016).

Strong spatial structure in silk-associated fungal communities has been demonstrated across small and large scales (Nazipi *et al.* 2021), so we expected to observe it here as well. Indeed, the fungal metacommunity responded more strongly to both spatial and environmental factors than the bacteria, suggesting that temperature and aridity also have a substantial localized effect on silk microbial assembly. Mean annual precipitation, mean annual temperature, and potential evapotranspiration have all been found to be generally good predictors of fungal alpha, beta, and gamma diversity, respectively (Mikryukov *et al.* 2023; Tedersoo *et al.* 2014). The environmental gradient here is suggestive; however, longer transects across a longer environmental gradient might yield stronger structuring power over microbial communities.

In contrast, the distance dependence of the silk bacterial metacommunity is not as strong as we might expect, given that both silks are constructed by spiders that rarely stray from the nest and maintain a strong social microbiome between generations (Rose *et al.* 2023b). For instance, in a strong distance-decay relationship, silks from the same site should be significantly different from silk comparisons made between colonies within the same transect or between transects. Here, the bacterial metacommunity shows that only the within-colony and between-transect comparisons are significantly different, suggesting a breakdown of distance-dependence at smaller scales. Previous analyses have also hinted at this pattern, where spatial structure of the silk microbiome between colonies breaks down at scales less than 500km (Busck *et al.* 2020; Keiser *et al.* 2019; Nazipi *et al.* 2021). Two forces may be responsible for driving this pattern. The first driver is bottom-up: the obligate, core microbiome of the spiders is small or nonexistent (Busck *et al.* 2020, 2022), and the social microbiome is easily disrupted by social fragmentation (Rose *et al.* 2023a); thus, spatial turnover may only be observable at very small scales (i.e. <100 m) where historical colony connections are most feasible. The alternative driver is top-down: High propagule pressure from cosmopolitan environmental taxa distributed across the region wash out the relationship between silk microbiomes within that area. Uncontrolled influx of microbes from high-diversity sources like soil can thus have major impacts on both the built environment and the social microbiome of its inhabitants.

Clearly, in this system, the soil microbiome has significant influence over the composition of the silk microbiome. However, it is interesting that this influence is realized in very different ways by the bacterial and fungal metacommunities. For instance, although neither the bacterial nor

fungal soil metacommunities showed any large-scale turnover with distance (distance-decay) or along the temperature and aridity gradient (environment-decay) fungal soil-silk relationships were stronger within colonies than between them. This suggests that a) soil fungal communities exhibit high spatial heterogeneity (much like soil bacteria (O'Brien *et al.* 2016)), and b) extremely localized fungal dispersal has a much more significant impact on nearby silks than long-distance dispersal.

The soil bacterial metacommunity, in contrast, demonstrated both no distance-decay relationship and only a very weak affinity to local silks relative to distant silks. This suggests that, compared to the soil fungi, soil bacteria are truly dispersal unlimited once airborne. The lack of any meaningful distance-decay relationship between soil bacteria and either silk type, despite high soil taxonomic contribution, supports the top-down perspective of high propagule pressure. Under the hypothesis of high dispersal, high loads of well-mixed soil bacteria caught in silk may influence nearby and distant nest communities equally. These taxa may be widely distributed due to low dispersal limitation of soil bacteria under extremely arid and windy conditions (Barberán *et al.* 2014; Choudoir *et al.* 2018).

The difference between bacterial and fungal cross-comparison patterns may be due to multiple factors related to fungal biology and life history traits, which may have significant impacts on the shape of their dispersal kernels: bacterial dispersal kernels may be more fat-tailed on average than fungal dispersal kernels (Golan & Pringle 2017; Jenkins *et al.* 2007). The standing assumption in the literature is that both bacteria and fungal spores are considered "dispersal unlimited" by virtue of their small size. However, fungal propagule size relative to bacteria may show relative more dispersal limitation (stronger distance-decay) in fungi than bacteria (De Bie *et al.* 2012; Wilkinson *et al.* 2012). There is also variation in fungal dispersal ability; for example, spores from mycorrhizal fungi are much larger than ascomycetes and basidiomycetes, and as a result, they do not hang in the air as long or travel as far (Egan *et al.* 2014; Peay *et al.* 2012). Generally longer lifespans in fungi also correspond with longer historical contingency in fungi than bacteria (Mennicken *et al.* 2020), although bacterial communities do exhibit some historical contingency too (Andersson *et al.* 2014).

Indirectly, the SourceTracker results concur with the idea that bacterial and fungal metacommunities here differ in degree of dispersal limitation. We included the SourceTracker analysis initially because of its application to sample contamination analysis over fairly large scales (Henry *et al.* 2016; Liu *et al.* 2018). In general, SourceTracker had an easier time classifying each bacterial ASV to its most likely source than it did each fungal ASV. In the bacteria, there was greater uncertainty with the so-called "Unknowns" than either the retreat or soil taxa; in the fungi, the greatest uncertainty was with the soil. This suggests that, in the fungal metacommunity, soil samples are each more directly paired to a particular capture sink than to the capture silk metacommunity as a whole. In contrast, several retreat fungi and bacteria appeared to be identifiable with high concordance between Gibbs samples. This suggests that these taxa may be silk or *S. dumicola* specialists that occupy silk and debris as a byproduct of their association with the host. In both bacterial and fungal metacommunities, the Unknown taxa are likely representative of either capture silk specialists or poorly distributed taxa. We suggest that the Unknown bacteria are more likely to be capture silk specialists, not only because they tend to be rare but also because the most abundant extrinsic taxa (*Geodermatophilus* and *Modestobacter*) are members of the family Geodermatophilaceae and commonly associated with soils (Normand *et al.* 2014). Likewise, we suggest that the Unknown fungi are more likely to be dispersal limited because they

were often highly abundant compared to the soil taxa. The most abundant Unknown or retreat taxa (*Aureobasidium,* Pleosporales sp.*,* and *Neocamarosporium*) are members of the class Dothideomycetes and most commonly found infecting plants or saprotrophic to decaying plant matter (Schoch *et al.* 2009) and may be most closely sourced from the plant acting as substrate to the nest.

There are two possible explanations for the discrepancy in classification power between bacterial and fungal datasets. The first explanation is biological: the fungi identified as Unknown may be immigrating from other, more significant sources than soil. One of these sources may be prey carcasses, as suggested previously (Keiser *et al.* 2019; Nazipi *et al.* 2021). The second explanation is based on the analytical structure of SourceTracker, which was originally designed to identify sources of sample contamination and quantify their contribution to sink sample composition (Knights *et al.* 2011). SourceTracker assumes that samples taken from a given source contain communities that are drawn from the same joint species distribution (Knights *et al.* 2011), which can be affected by dispersal limitation, gradients of abiotic factors, and/or biotic interactions (Leibold *et al.* 2021). If these communities are not equally governed by the same underlying ecological processes, the resulting pattern is high uncertainty around assignments to one or more of the given sources -- in this case, soil.

To our knowledge, SourceTracker has not been applied to a dataset of this geographic scale before. Previous studies applying it have been largely limited to single experimental setups in the lab (Pedersen *et al.* 2015), or to exploring waterborne contamination across broader scales in the field (e.g. (Bauza *et al.* 2019; Henry *et al.* 2016; Liu *et al.* 2018; Tian *et al.* 2024)]. In both cases, the assumption is that dispersal between samples is high. We find that its assumptions about the nature of the distribution underlying the relationship between sources and sinks make it an unexpectedly useful tool for discriminating dispersal specialists on very large scales. Other methods, such as those by Stegen et al (Stegen *et al.* 2013, 2015), are perhaps better approaches for parsing homogenizing dispersal from dispersal limitation within one type of sample (i.e. soils) but are not designed for estimating relationships between sample types.

Together, these different lines of evidence indicate that the bacterial and fungal metacommunities in this system take on different network structures. Based on our analysis, we hypothesize that the fungal metacommunity takes on a multi-layer network-like structure, where the strongest links occur within sample type, and additional links between sample types are moderated by distance. In contrast, we hypothesize that the bacterial metacommunity assumes a modular network-like structure, where samples (the nodes) are strongly linked within each sample type but weakly linked between types, and link strength is not influenced by geographical distance. This work explores the baseline for the relationship between the built environment and extrinsic microbial sources in this system. Future work should address how the differences in bacterial and fungal metacommunity structure influence the social microbiome and health of hosts. Different network structures are known to influence microbial transmission (Shirley & Rushton 2005) and may be factors in pathogen accumulation and nest decline in *S. dumicola* (Busck *et al.* 2022). Alternatively, how these networks influence compositional changes to the host- and nest-associated microbiome over time may locally alter host fitness and survival patterns (Mueller *et al.* 2020).

Acknowledgements

We would like to thank… and our reviewers for their constructive feedback.

Author contributions

CNK funded the project and designed/executed the field work and sample collection with PRM. STC organized and performed sample extraction, processing, and data collection. KJMT designed and executed the data analysis. KJMT lead the manuscript writing with STC, PRM, MAL, and CNK all contributing to the writing. MAL provided support funding and conceptual guidance to KJMT during the analysis phase.

Declaration of interests

Authors declare no competing interests.

Funding

KJMT was funded by NSF 2025118

References

Ainsworth, C., Slotow, R., Crouch, T. & Lubin, Y. (2002). Lack of task differentiation during prey capture in the group living spider Stegodyphus mimosarum (Araneae, Eresidae). *arac*, 30, 39–46.

Andersson, M.G.I., Berga, M., Lindström, E.S. & Langenheder, S. (2014). The spatial structure of bacterial communities is influenced by historical environmental conditions. *Ecology*, 95, 1134–1140.

Astorga, A., Oksanen, J., Luoto, M., Soininen, J., Virtanen, R. & Muotka, T. (2012). Distance decay of similarity in freshwater communities: do macro- and microorganisms follow the same rules? *Global Ecology and Biogeography*, 21, 365–375.

Aviles, L. (1997). Causes and consequences of cooperation and permanent sociality in spiders. *The evolution of social behaviour in insects and arachnids*.

Barberán, A., Henley, J., Fierer, N. & Casamayor, E.O. (2014). Structure, inter-annual recurrence, and global-scale connectivity of airborne microbial communities. *Science of The Total Environment*, 487, 187–195.

Bauza, V., Madadi, V., Ocharo, R.M., Nguyen, T.H. & Guest, J.S. (2019). Microbial Source Tracking Using 16S rRNA Amplicon Sequencing Identifies Evidence of Widespread Contamination from Young Children's Feces in an Urban Slum of Nairobi, Kenya. *Environ. Sci. Technol.*, 53, 8271–8281.

Bosch, T.C.G., Wigley, M., Colomina, B., Bohannan, B., Meggers, F., Amato, K.R., *et al.* (2024). The potential importance of the built-environment microbiome and its impact on human health. *Proceedings of the National Academy of Sciences*, 121, e2313971121.

Busck, M.M., Lund, M.B., Bird, T.L., Bechsgaard, J.S., Bilde, T. & Schramm, A. (2022). Temporal and spatial microbiome dynamics across natural populations of the social spider Stegodyphus dumicola. *FEMS Microbiology Ecology*, 98, fiac015.

Busck, M.M., Settepani, V., Bechsgaard, J., Lund, M.B., Bilde, T. & Schramm, A. (2020). Microbiomes and Specific Symbionts of Social Spiders: Compositional Patterns in Host Species, Populations, and Nests. *Frontiers in Microbiology*, 11.

Cassidy, S.T., Pope, A., Missigman, N., Taylor, K.J.M., Haufiku, M., Kavili, T., *et al.* (2025). Exploring the effects of horizontal pathogen transmission on mortality and behaviour in a cooperatively breeding spider. *Animal Behaviour*, 222, 123113.

Choudoir, M.J., Barberán, A., Menninger, H.L., Dunn, R.R. & Fierer, N. (2018). Variation in range size and dispersal capabilities of microbial taxa. *Ecology*, 99, 322–334.

Christenson, T.E. (1984). Behaviour of colonial and solitary spiders of the theridiid species *Anelosimus eximius*. *Animal Behaviour*, 32, 725–734.

Crouch, T. & Lubin, Y. (2001). Population stability and extinction in a social spider Stegodyphus mimosarum (Araneae: Eresidae). *Biological Journal of the Linnean Society*, 72, 409–417.

De Bie, T., De Meester, L., Brendonck, L., Martens, K., Goddeeris, B., Ercken, D., *et al.* (2012). Body size and dispersal mode as key traits determining metacommunity structure of aquatic organisms. *Ecology Letters*, 15, 740–747.

Dray, S., Legendre, P. & Peres-Neto, P.R. (2006). Spatial modelling: a comprehensive framework for principal coordinate analysis of neighbour matrices (PCNM). *Ecological Modelling*, 196, 483–493.

Egan, C., Li, D.-W. & Klironomos, J. (2014). Detection of arbuscular mycorrhizal fungal spores in the air across different biomes and ecoregions. *Fungal Ecology*, Fungal ecology beyond boundaries: from communities to the globe, 12, 26–31.

Feng, M., Tripathi, B.M., Shi, Y., Adams, J.M., Zhu, Y.-G. & Chu, H. (2019). Interpreting distance-decay pattern of soil bacteria via quantifying the assembly processes at multiple spatial scales. *MicrobiologyOpen*, 8, e00851.

Fernandez-Fournier, P. & Avilés, L. (2018). Environmental filtering and dispersal as drivers of metacommunity composition: complex spider webs as habitat patches. *Ecosphere*, 9, e02101.

Fick, S.E. & Hijmans, R.J. (2017). WorldClim 2: new 1-km spatial resolution climate surfaces for global land areas. *International Journal of Climatology*, 37, 4302–4315.

Gilbert, B. & Lechowicz, M.J. (2004). Neutrality, niches, and dispersal in a temperate forest understory. *Proceedings of the National Academy of Sciences*, 101, 7651–7656.

Golan, J.J. & Pringle, A. (2017). Long-Distance Dispersal of Fungi. *Microbiology Spectrum*, 5, 10.1128/microbiolspec.funk-0047–2016.

Guénard, G. & Legendre, P. (2022). Hierarchical Clustering with Contiguity Constraint in R. *Journal of Statistical Software*, 103, 1–26.

Henry, R., Schang, C., Coutts, S., Kolotelo, P., Prosser, T., Crosbie, N., *et al.* (2016). Into the deep: Evaluation of SourceTracker for assessment of faecal contamination of coastal waters. *Water Research*, 93, 242–253.

Hill, M.S. & Gilbert, J.A. (2023). Microbiology of the built environment: harnessing human-associated built environment research to inform the study and design of animal nests and enclosures. *Microbiology and Molecular Biology Reviews*, 87, e00121-21.

Jenkins, D.G., Brescacin, C.R., Duxbury, C.V., Elliott, J.A., Evans, J.A., Grablow, K.R., *et al.* (2007). Does size matter for dispersal distance? *Global Ecology and Biogeography*, 16, 415–425.

Keiser, C.N., Hammer, T.J. & Pruitt, J.N. (2019). Social spider webs harbour largely consistent bacterial communities across broad spatial scales. *Biology Letters*, 15, 20190436.

Keiser, C.N., Howell, K.A., Pinter-Wollman, N. & Pruitt, J.N. (2016). Personality composition alters the transmission of cuticular bacteria in social groups. *Biology Letters*, 12, 20160297.

Kembel, S.W., Cowan, P.D., Helmus, M.R., Cornwell, W.K., Morlon, H., Ackerly, D.D., *et al.* (2010). Picante: R tools for integrating phylogenies and ecology. *Bioinformatics*, 26, 1463–1464.

Knights, D. (2016). SourceTracker for R.

Knights, D., Kuczynski, J., Charlson, E.S., Zaneveld, J., Mozer, M.C., Collman, R.G., *et al.* (2011). Bayesian community-wide culture-independent microbial source tracking. *Nat Methods*, 8, 761–763.

Legendre, P. (2008). Studying beta diversity: ecological variation partitioning by multiple regression and canonical analysis. *Journal of Plant Ecology*, 1, 3–8.

Legendre, P., Borcard, D. & Peres-Neto, P.R. (2005). Analyzing Beta Diversity: Partitioning the Spatial Variation of Community Composition Data. *Ecological Monographs*, 75, 435–450.

Leibold, M.A. & Chase, J.M. (2017). *Metacommunity Ecology*. *Metacommunity Ecology, Volume 59*, Monographs in Population Biology. Princeton University Press.

Leibold, M.A., Rudolph, F.J., Blanchet, F.G., De Meester, L., Gravel, D., Hartig, F., *et al.* (2021). The internal structure of metacommunities. *Oikos*, 2022.

Li, S., Yang, Z., Hu, D., Cao, L. & He, Q. (2021). Understanding building-occupant-microbiome interactions toward healthy built environments: A review. *Front. Environ. Sci. Eng.*, 15, 65.

Liu, G., Zhang, Y., van der Mark, E., Magic-Knezev, A., Pinto, A., van den Bogert, B., *et al.* (2018). Assessing the origin of bacteria in tap water and distribution system in an unchlorinated drinking water system by SourceTracker using microbial community fingerprints. *Water Research*, 138, 86–96.

Locey, K.J., Muscarella, M.E., Larsen, M.L., Bray, S.R., Jones, S.E. & Lennon, J.T. (2020). Dormancy dampens the microbial distance–decay relationship. *Philosophical Transactions of the Royal Society B: Biological Sciences*, 375, 20190243.

Lucas, J.M., Madden, A.A., Penick, C.A., Epps, M.J., Marting, P.R., Stevens, J.L., *et al.* (2019). Azteca ants maintain unique microbiomes across functionally distinct nest chambers. *Proceedings of the Royal Society B: Biological Sciences*, 286, 20191026.

Martinez Arbizu, P. (2020). pairwiseAdonis: Pairwise multilevel comparison using adonis.

Martiny, J.B.H., Bohannan, B.J.M., Brown, J.H., Colwell, R.K., Fuhrman, J.A., Green, J.L., *et al.* (2006). Microbial biogeography: putting microorganisms on the map. *Nat Rev Microbiol*, 4, 102–112.

Mennicken, S., Kondratow, F., Buralli, F., Manzi, S., Andrieu, E., Roy, M., *et al.* (2020). Effects of Past and Present-Day Landscape Structure on Forest Soil Microorganisms. *Frontiers in Ecology and Evolution*, 8.

Mikryukov, V., Dulya, O., Zizka, A., Bahram, M., Hagh-Doust, N., Anslan, S., *et al.* (2023). Connecting the multiple dimensions of global soil fungal diversity. *Science Advances*, 9, eadj8016.

Miller, E.T., Svanbäck, R. & Bohannan, B.J.M. (2018). Microbiomes as Metacommunities: Understanding Host-Associated Microbes through Metacommunity Ecology. *Trends in Ecology & Evolution*, 33, 926–935.

Mueller, E.A., Wisnoski, N.I., Peralta, A.L. & Lennon, J.T. (2020). Microbial rescue effects: How microbiomes can save hosts from extinction. *Functional Ecology*, 34, 2055–2064.

Nazipi, S., Elberg, C.L., Busck, M.M., Lund, M.B., Bilde, T. & Schramm, A. (2021). The bacterial and fungal nest microbiomes in populations of the social spider Stegodyphus dumicola. *Systematic and Applied Microbiology*, 44, 126222.

Normand, P., Daffonchio, D. & Gtari, M. (2014). The Family Geodermatophilaceae. In: *The Prokaryotes: Actinobacteria* (eds. Rosenberg, E., DeLong, E.F., Lory, S., Stackebrandt, E. & Thompson, F.). Springer Berlin Heidelberg, Berlin, Heidelberg, pp. 361–379.

O'Brien, S.L., Gibbons, S.M., Owens, S.M., Hampton-Marcell, J., Johnston, E.R., Jastrow, J.D., *et al.* (2016). Spatial scale drives patterns in soil bacterial diversity. *Environmental Microbiology*, 18, 2039–2051.

Oksanen, J., Simpson, G.L., Blanchet, F.G., Kindt, R., Legendre, P., Minchin, P.R., *et al.* (2022). *vegan: Community Ecology Package*.

Peay, K.G., Schubert, M.G., Nguyen, N.H. & Bruns, T.D. (2012). Measuring ectomycorrhizal fungal dispersal: macroecological patterns driven by microscopic propagules. *Molecular Ecology*, 21, 4122–4136.

Pedersen, M.W., Overballe-Petersen, S., Ermini, L., Sarkissian, C.D., Haile, J., Hellstrom, M., *et al.* (2015). Ancient and modern environmental DNA. *Philosophical Transactions of the Royal Society B: Biological Sciences*, 370, 20130383.

Peres-Neto, P.R. & Legendre, P. (2010). Estimating and controlling for spatial structure in the study of ecological communities. *Global Ecology and Biogeography*, 19, 174–184.

Peres-Neto, P.R., Legendre, P., Dray, S. & Borcard, D. (2006). Variation Partitioning of Species Data Matrices: Estimation and Comparison of Fractions. *Ecology*, 87, 2614–2625.

QGIS Development Team, A. & others. (2024). QGIS geographic information system. *Open source geospatial foundation project*.

R Core Team. (2024). *R: A Language and Environment for Statistical Computing*. R Foundation for Statistical Computing, Vienna, Austria.

Ranjard, L., Dequiedt, S., Chemidlin Prévost-Bouré, N., Thioulouse, J., Saby, N.P.A., Lelievre, M., *et al.* (2013). Turnover of soil bacterial diversity driven by wide-scale environmental heterogeneity. *Nat Commun*, 4, 1434.

Rose, C., Lund, M.B., Schramm, A., Bilde, T. & Bechsgaard, J. (2023a). Does ecological drift explain variation in microbiome composition among groups in a social host species? *Journal of Evolutionary Biology*, 36, 1684–1694.

Rose, C., Lund, M.B., Søgård, A.M., Busck, M.M., Bechsgaard, J.S., Schramm, A., *et al.* (2023b). Social transmission of bacterial symbionts homogenizes the microbiome within and across generations of group-living spiders. *ISME COMMUN.*, 3, 1–10.

Sarkar, A., Harty, S., Johnson, K.V.-A., Moeller, A.H., Archie, E.A., Schell, L.D., *et al.* (2020). Microbial transmission in animal social networks and the social microbiome. *Nat Ecol Evol*, 4, 1020–1035.

Sarkar, A., McInroy, C.J.A., Harty, S., Raulo, A., Ibata, N.G.O., Valles-Colomer, M., *et al.* (2024). Microbial transmission in the social microbiome and host health and disease. *Cell*, 187, 17–43.

Schoch, C.L., Crous, P.W., Groenewald, J.Z., Boehm, E.W.A., Burgess, T.I., de Gruyter, J., *et al.* (2009). A class-wide phylogenetic assessment of Dothideomycetes. *Stud Mycol*, 64, 1-15S10.

Settepani, V., Schou, M.F., Greve, M., Grinsted, L., Bechsgaard, J. & Bilde, T. (2017). Evolution of sociality in spiders leads to depleted genomic diversity at both population and species levels. *Molecular Ecology*, 26, 4197–4210.

Shirley, M.D.F. & Rushton, S.P. (2005). The impacts of network topology on disease spread. *Ecological Complexity*, 2, 287–299.

Smith, D., Van Rijn, S., Henschel, J., Bilde, T. & Lubin, Y. (2009). Amplified fragment length polymorphism fingerprints support limited gene flow among social spider populations. *Biological Journal of the Linnean Society*, 97, 235–246.

Soininen, J., McDonald, R. & Hillebrand, H. (2007). The distance decay of similarity in ecological communities. *Ecography*, 30, 3–12.

Soydaner, A.L. (2013). Compensating for the Consequences of Group-living in the Cooperative Spider Stegodyphus dumicola. *MSc. Arhus University*.

Stegen, J.C., Lin, X., Fredrickson, J.K., Chen, X., Kennedy, D.W., Murray, C.J., *et al.* (2013). Quantifying community assembly processes and identifying features that impose them. *The ISME Journal*, 7, 2069–2079.

Stegen, J.C., Lin, X., Fredrickson, J.K. & Konopka, A.E. (2015). Estimating and mapping ecological processes influencing microbial community assembly. *Front. Microbiol.*, 0.

Stegen, J.C., Lin, X., Konopka, A.E. & Fredrickson, J.K. (2012). Stochastic and deterministic assembly processes in subsurface microbial communities. *The ISME Journal*, 6, 1653–1664.

Tedersoo, L., Bahram, M., Põlme, S., Kõljalg, U., Yorou, N.S., Wijesundera, R., *et al.* (2014). Global diversity and geography of soil fungi. *Science*, 346, 1256688.

Tian, Y., Han, Z., Su, D., Luan, X., Yu, L., Tian, Z., *et al.* (2024). Assessing impacts of municipal wastewater treatment plant upgrades on bacterial hazard contributions to the receiving urban river using SourceTracker. *Environmental Pollution*, 342, 123075.

Wilkins, D., Leung, M.H. & Lee, P.K. (2016). Indoor air bacterial communities in H ong K ong households assemble independently of occupant skin microbiomes. *Environmental Microbiology*, 18, 1754–1763.

719 Wilkinson, D.M., Koumoutsaris, S., Mitchell, E.A.D. & Bey, I. (2012). Modelling the effect of
720 size on the aerial dispersal of microorganisms. *Journal of Biogeography*, 39, 89–97.

721 Zomer, R.J., Bossio, D.A., Trabucco, A., Yuanjie, L., Gupta, D.C. & Singh, V.P. (2007). *Trees*
722 *and water: smallholder agroforestry on irrigated lands in Northern India*. IWMI.

723 Zomer, R.J., Trabucco, A., Bossio, D.A. & Verchot, L.V. (2008). Climate change mitigation: A
724 spatial analysis of global land suitability for clean development mechanism afforestation
725 and reforestation. *Agriculture, ecosystems & environment*, 126, 67–80.

726

Supplemental information

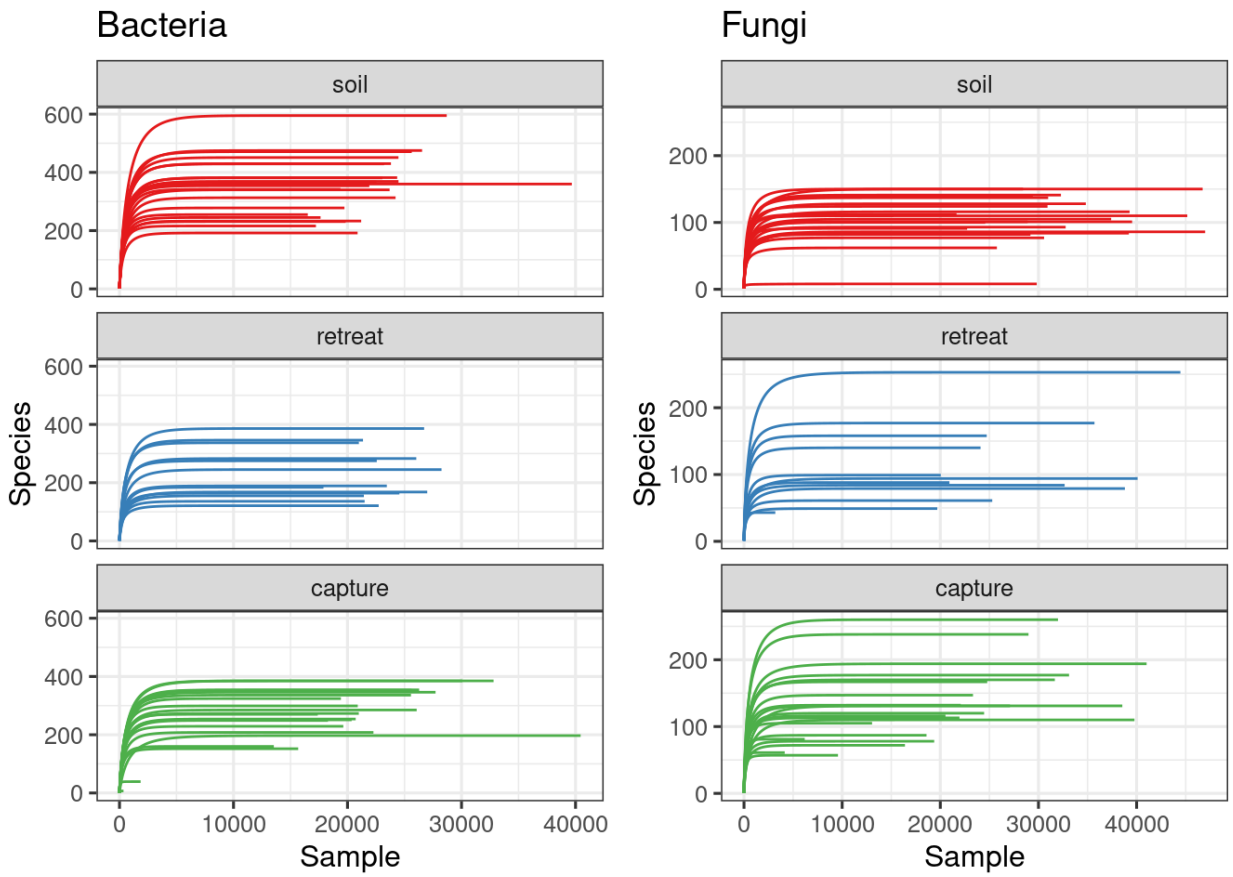

Figure S1. Rarefaction curves for bacterial (left) and fungal (right) communities from soil, (top), retreat silk (middle) and capture silk (bottom) samples. Curves were generated with a sample size of 250 taxa.

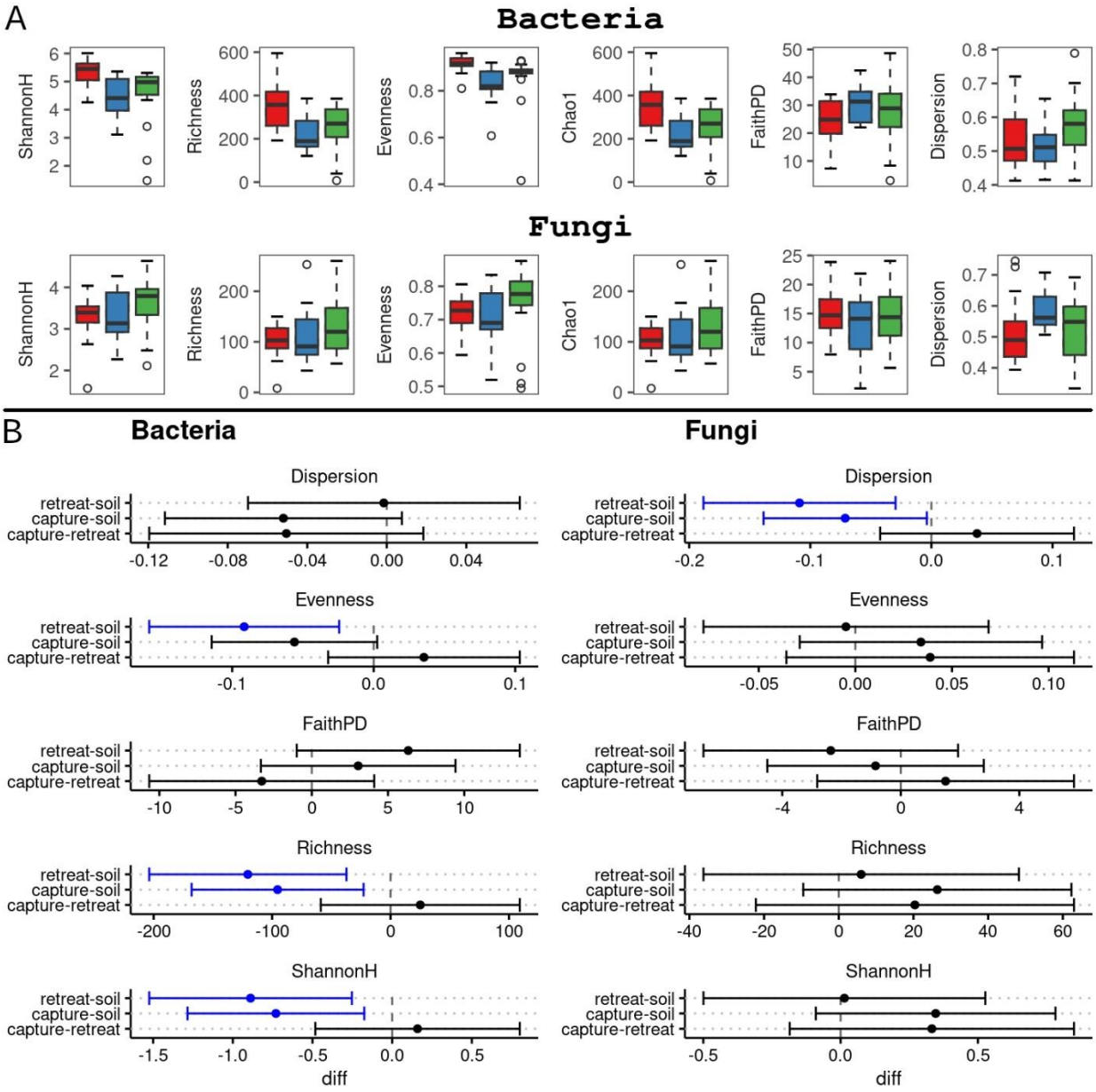

Figure S2. All diversity metrics calculated for bacterial and fungal communities: Shannon's H, Richness, Evenness, Chao1, Faith's PD, beta dispersion. A) Boxplots show the values of each metric for each sample type. B) Tukey HSD results for pairwise ANOVA comparisons between the sample types for each metric. Blue lines indicate those differences between groups that are statistically different from 0.

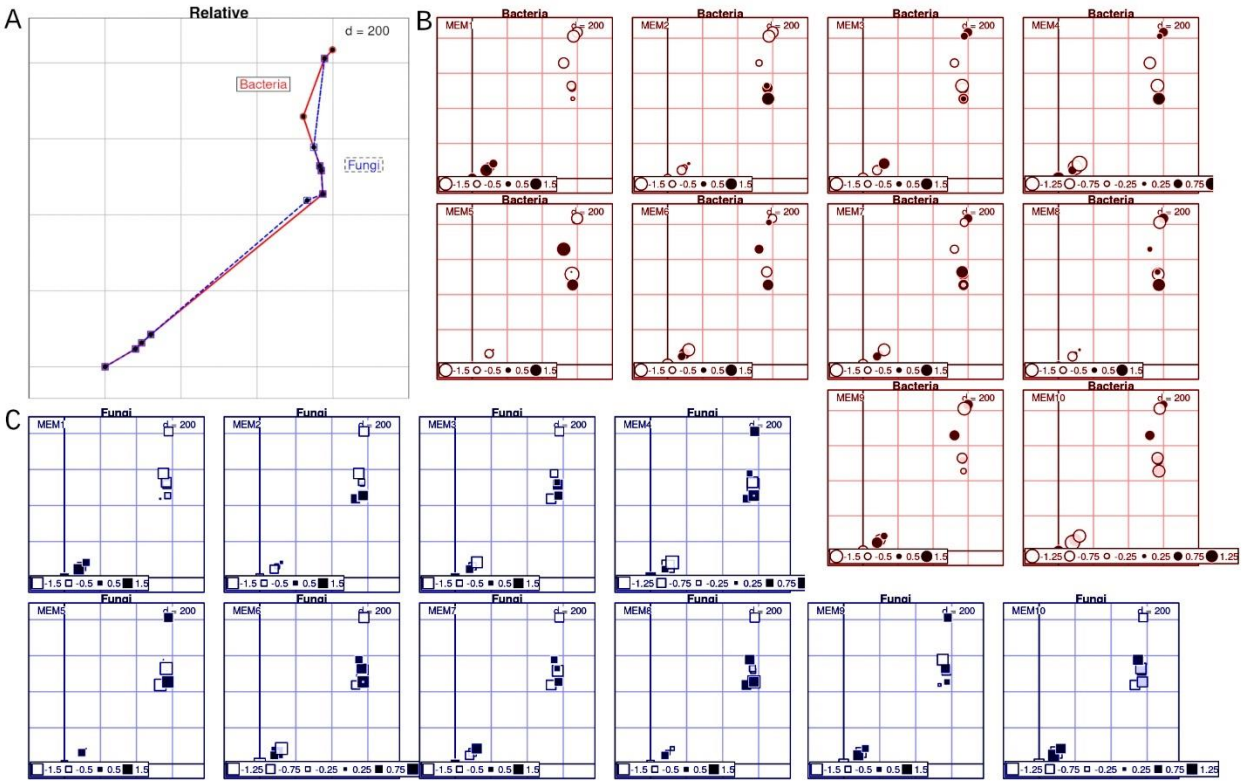

Figure S3. Building the Moran Eigenvector Map from a relative neighbor network. A) The relative neighbor network for bacterial sites (N=11, indicated in red) and fungal sites (N=11, indicated in blue). B) MEMs 1-10 for bacterial sites. C) MEMs 1-10 for fungal sites.

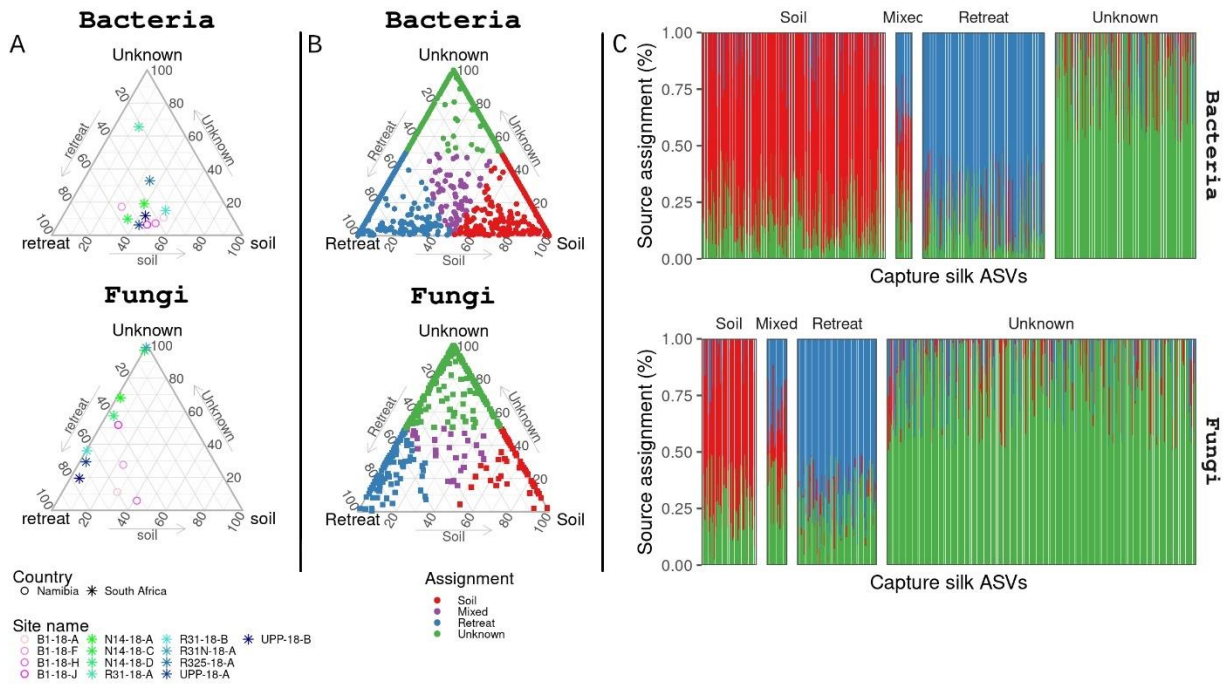

Figure S4. A) Ternary plots showing the mean source assignment of each site averaged across all taxa. Most bacterial communities are dominated by retreat or soil taxa. Most fungal communities are dominated by retreat or Unknown taxa. B,C) Source assignment for each ASV, segregated by the average proportion of the assignment exceeding 50%. B) Ternary plots show the mean proportion of reads drawn by the Gibbs sampler for each ASV. C) Bar graph shows the mean proportions for each ASV visualized a different way.

Table S1. Multiple regression of binary Bray-Curtis similarity of bacterial microbiota from each sample type (retreat silk, capture silk, soil) as a function of geographical distance (Latitude x Longitude) and environmental dissimilarity (Temp x Aridity)

		Coefficients	*Std.Err*	*t Stat*	*P-value*	R^2	*Adj.* R^2	*Std.Err*	*F Stat*	*P-value*	*N*
Retreat	Intercept	0.4895	3.42E-02	14.31	<0.001 ***	0.41	0.38	0.11	11.98	<0.001 ***	55
	Distance	-7.49E-04	1.64E-04	-4.56	<0.001 ***						
	Transect	-1.48E-02	1.23E-01	-0.12	0.90						
	Distance:Transect	4.72E-04	2.26E-04	2.09	0.04 *						
	Intercept	0.4953	3.42E-02	14.49	<0.001 ***	0.44	0.40	0.10	13.13	<0.001 ***	55
	Environment	-7.56E-02	1.60E-02	-4.72	<0.001 ***						
	Transect	-1.59E-01	5.13E-02	-3.09	0.003 **						
	Env:Transect	3.12E-02	2.61E-02	1.20	0.24						
Capture	Intercept	0.4630	2.05E-02	22.55	<0.001 ***	0.26	0.21	0.06	5.92	<0.001 ***	55
	Distance	-2.55E-04	9.87E-05	-2.58	0.013 *						
	Transect	8.45E-02	7.38E-02	1.14	0.26						
	Distance:Transect	3.34E-05	1.36E-04	0.25	0.81						
	Intercept	0.4691	1.81E-02	25.96	<0.001 ***	0.45	0.41	0.05	13.69	<0.001 ***	55
	Environment	-2.81E-02	8.46E-03	-3.32	0.002 **						
	Transect	-5.16E-03	2.71E-02	-0.19	0.85						
	Env:Transect	-2.39E-02	1.38E-02	-1.74	0.09						
Soil	Intercept	0.3603	2.97E-02	12.11	<0.001 ***	0.07	0.01	0.09	1.21	0.319	55
	Distance	-2.47E-04	1.43E-04	-1.72	0.09						
	Transect	-4.09E-02	1.07E-01	-0.38	0.70						
	Distance:Transect	2.20E-04	1.96E-04	1.12	0.27						
	Intercept	0.3537	3.02E-02	11.71	<0.001 ***	0.07	0.02	0.09	1.34	0.268	55
	Environment	-2.00E-02	1.41E-02	-1.41	0.16						
	Transect	-1.96E-02	4.53E-02	-0.43	0.67						
	Env:Transect	-1.56E-03	2.30E-02	-0.07	0.95						

***p < 0.001; **p < 0.01; *p < 0.05

Table S2.

Table S2. Multiple regression of binary Bray-Curtis similarity of fungal microbiota from each sample type (retreat silk, capture silk, soil) as a function of geographical distance (Latitude x Longitude) and environmental dissimilarity (Temp x Aridity)

		Coefficients	*Std.Err*	*t Stat*	*P-value*	*R^2*	*Adj. R^2*	*Std.Err*	*F Stat*	*P-value*	*N*
Retreat	Intercept	0.5671	2.80E-02	20.28	<0.001 ***	0.49	0.46	0.10	16.43	<0.001 ***	55
	Distance	-6.75E-04	1.66E-04	-4.07	<0.001 ***						
	Transect	-6.20E-02	1.20E-01	-0.52	0.61						
	Distance:Transect	4.37E-04	2.34E-04	1.87	0.07						
	Intercept	0.5441	3.13E-02	17.39	<0.001 ***	0.41	0.37	0.10	11.60	<0.001 ***	55
	Environment	-3.79E-02	1.46E-02	-2.60	0.012 *						
	Transect	-1.66E-01	4.68E-02	-3.55	<0.001 ***						
	Env:Transect	1.25E-02	2.38E-02	0.53	0.60						
Capture	Intercept	0.5719	1.72E-02	33.23	<0.001 ***	0.62	0.60	0.06	27.95	<0.001 ***	55
	Distance	-6.47E-04	1.02E-04	-6.33	<0.001 ***						
	Transect	1.16E-01	7.38E-02	1.58	0.12						
	Distance:Transect	2.43E-04	1.44E-04	1.68	0.10						
	Intercept	0.5718	1.72E-02	33.18	<0.001 ***	0.65	0.62	0.06	30.99	<0.001 ***	55
	Environment	-4.94E-02	8.02E-03	-6.16	<0.001 ***						
	Transect	-8.60E-02	2.58E-02	-3.33	0.002 **						
	Env:Transect	-2.64E-03	1.31E-02	-0.20	0.84						
Soil	Intercept	0.3978	2.43E-02	16.35	<0.001 ***	0.07	0.01	0.08	1.21	0.318	55
	Distance	-2.08E-04	1.45E-04	-1.44	0.16						
	Transect	-1.08E-01	1.04E-01	-1.04	0.30						
	Distance:Transect	2.90E-04	2.04E-04	1.42	0.16						
	Intercept	0.3979	2.52E-02	15.78	<0.001 ***	0.06	0.01	0.08	1.15	0.346	55
	Environment	-1.60E-02	1.17E-02	-1.36	0.18						
	Transect	-3.76E-02	3.77E-02	-1.00	0.32						
	Env:Transect	6.95E-03	1.92E-02	0.36	0.72						

***p < 0.001; **p < 0.01; *p < 0.05;